British Geological Survey
NATURAL ENVIRONMENT RESEARCH COUNCIL

A method to generate fracture patterns with statistical scaling and spatial distributions

Programme: Geochemistry, Mineralogy and Hydrogeology
BGS Research Report CR/03/89N

Enru Liu and Serafeim Vlastos, British Geological Survey, Edinburgh
Zhongjie Zhang, Institute of Geology & Geophysics, Chinese Academy of Sciences
Antoni E. Milodowski, British Geological Survey, Keyworth

British Geological Survey,
Murchison House, West Mains Road,
Edinburgh EH9 3LA, United Kingdom
Tel. 0131 650 0362; Fax. 0131 667 1877
Email. E.Liu@bgs.ac.uk

The full range of Survey publications is available from the BGS Sales Desks at Nottingham and Edinburgh; see contact details below or shop online at www.thebgs.co.uk

The London Information Office maintains a reference collection of BGS publications including maps for consultation.

The Survey publishes an annual catalogue of its maps and other publications; this catalogue is available from any of the BGS Sales Desks.

The British Geological Survey carries out the geological survey of Great Britain and Northern Ireland (the latter as an agency service for the government of Northern Ireland), and of the surrounding continental shelf, as well as its basic research projects. It also undertakes programmes of British technical aid in geology in developing countries as arranged by the Department for International Development and other agencies.

The British Geological Survey is a component body of the Natural Environment Research Council.

Keyworth, Nottingham NG12 5GG

☎ 0115-936 3241 Fax 0115-936 3488
e-mail: sales@bgs.ac.uk
www.bgs.ac.uk
Shop online at: www.thebgs.co.uk

Murchison House, West Mains Road, Edinburgh EH9 3LA

☎ 0131-667 1000 Fax 0131-668 2683
e-mail: scotsales@bgs.ac.uk

London Information Office at the Natural History Museum (Earth Galleries), Exhibition Road, South Kensington, London SW7 2DE

☎ 020-7589 4090 Fax 020-7584 8270
☎ 020-7942 5344/45 email: bgslondon@bgs.ac.uk

Forde House, Park Five Business Centre, Harrier Way, Sowton, Exeter, Devon EX2 7HU

☎ 01392-445271 Fax 01392-445371

Geological Survey of Northern Ireland, 20 College Gardens, Belfast BT9 6BS

☎ 028-9066 6595 Fax 028-9066 2835

Maclean Building, Crowmarsh Gifford, Wallingford, Oxfordshire OX10 8BB

☎ 01491-838800 Fax 01491-692345

Parent Body
Natural Environment Research Council, Polaris House,
North Star Avenue, Swindon, Wiltshire SN2 1EU

☎ 01793-411500 Fax 01793-411501
www.nerc.ac.uk

Contents Page

Keywords: fracture pattern, fractal distribution, finite difference method, seismic waves, FORTRAN

A method to generate fracture patterns with statistical scaling and spatial distributions

E. Liu [a], S. Vlastos [a,1], Z.J. Zhang [b] & A.E. Milodowski [a]

[a] *British Geological Survey, Murchison House, West Mains Road, Edinburgh EH9 3LA, UK (email: E.Liu@bgs.ac.uk)*

[b] *Institute of Geology & Geophysics, Chinese Academy of Sciences, 11A Datun Road, Beijing 100101, China*

Abstract

A method for the generation of realistic fracture patterns is presented. The compute program, written in FORTRAN 77, follows an approach of the scaling of natural fractures. The properties of spatial and size distributions are controlled by the statistical distribution. It is a fast and efficient way to generate various fractured patterns with realistic spatial distributions, including power-law or fractal distribution of fracture sizes. The patterns created by the program have been applied to model seismic wave propagation, and fluid flow simulation in fractured rocks. Some sample patterns are presented in this paper to demonstrate the flexibility of this simple, and efficient method.

Key words: Fracture pattern, fractal distribution, finite-difference methods, wave propagation, FORTRAN 77.

1 Introduction

Scaling in fracture systems has become an active field of research in the last 25 years motivated by practical applications (e.g. Bonnet et al., 2001). In the case of the hydrocarbon industry, scaling laws provide a key to the prediction of the nature of subseismic fracturing (below the limit of seismic resolution), which can significantly influence fluid flow in reservoirs and cap rock quality, from seismically resolved faults. The numerous studies of fracture-system scaling in

[1] Also at: Department of Geology & Geophysics, University of Edinburgh, Grant Institute, West Mains Road, Edinburgh EH9 3JW, UK

the literature do indeed suggest that scaling laws exist in nature. It is also indicated, however, that such scaling laws must be used with caution due to the physical influences that govern their validity. In recent years the power law distribution has been increasingly employed to describe the frequency distribution of fracture properties and geometry. However, a power law is not an appropriate model in all cases, and other distributions that have been used include the log normal, gamma, and exponential laws. In the program presented here we have a choice between a power law, a random uniform, a Gaussian, an exponential, and a Gamma distribution. Other distributions may easily be included without additional difficulty.

The generation of synthetic fracture populations and patterns has become well-established using sophisticated cellular automatons. Those models can create detailed patterns of development of a population of fractures involving nucleation, growth, branching, interaction and coalescence (Cowie et al., 1993; Cowie et al., 1995; An and Sammis, 1996; Narteau et al., 2000). Such a detailed discussion and representation of fracture generation, evolution and formation of certain patterns are beyond the scope of the program presented here. Instead, we present a simple, but yet efficient method to generate realistic fracture patterns for applications, for example, in the forward modelling of wave propagation and fluid flow simulation in fractured media. Though the created fracture patterns do not obey to any law that controls their evolution, their spatial or size pattern follows a statistical distribution defined by the user.

2 Generation of fracture distributions

In this section, we will describe the procedure and the algorithm that are used to create the different fracture patterns. The algorithm can generate four different spatial distributions of fractures, (a) random uniform, (b) Gaussian, (c) exponential, and (d) gamma. The certain distributions are chosen as being the most commonly demonstrated patterns in fractured rock. For instance, in continental rocks and in the vicinity of mid-oceanic ridges fracture growth results from a uniform stress distribution (Dershowitz and Einstein, 1988), and propagation of fratures can be compared to a Poisson process (Cruden, 1977) resulting in an exponential distribution. Also the gamma distribution is a power law with an exponential tail and is in common use in fault and earthquake statistics and seismic hazard assessment (Main, 1996; Sornette and Sornette, 1999).

The algorithm utilizes the different random number generators (e.g. Press et al., 1997; or supplied by users), that varies according to the distribution defined by users. For each distribution, the generator is applied once to give

x-coordinates, and completely independently once more to give z-coordinates. Both x- and z-coordinates are then normalised to the grid size of the model. Those pairs of x- and z-coordinates are the centres of the distributed fractures. The resulting distribution of fractures, without any alterations, is the parent spatial distribution. The size and orientation of the fractures are given as inputs to the algorithm. Subsequently, the algorithm examines the fractures for any overlapping cases. We define overlapping as the case where the distance between the centres of two fractures is less than a predefined value. The testing of overlapping is optional and depends on users' choice. After that, the remaining number of distributed fractures is counted. If that number is less than the desired number, the resulting distribution of fractures is rejected. The number of fractures following the parent spatial distribution is raised by a number chosen by users (the default number is set to 5). A new group of fractures, spatially distributed according to the parent distribution, is chosen. The new group of fractures follows the same procedure that described above. This process continues until the desired number of non-overlapping spatially distributed fractures is reached. A flow chart of the filtering algorithm is presented in Fig. 1. The final spatial distribution of the fractures is a result of the parent distribution after applying data filtering, so we call this the daughter spatial distribution. The spatial correlation in the daughter population is then determined by the two-point correlation function of the fracture centre locations in two dimensions. The two-point correlation function $C(r)$, for each distribution is defined as, $C(r) = \frac{1}{N^2} N_d(r)$, where N is the total number of points and N_d is the number of pairs of points whose distance is less than r (Hentschel and Proccacia, 1983).

3 Examples

We present three examples, that exhibit the use of the presented program in the generation of fracture distributions which have different statistical properties. For each example we also show the statistical properties. We present a case of parallel fractures of the same size that have different spatial distributions, a case of parallel fractures that have different sizes, and fractures at arbitrary angles.

3.1 Spatial distributions

The first example is given in Fig. 2, in which we present four different simulations of fracture distributions. In each model, there are 100 fractures distributed in a 1280 x 1280 m^2 area. The parent distributions for the fracture centre spacing are (a) random uniform, (b) Gaussian, (c) exponential, and (d)

Gamma. In this simulation, each fracture has the same length, $2a = 30m$. As we can see from Fig. 2 due to statistical distribution, fractures are clustered in models (b) and (c), whereas they are uniformly distributed or more scattered in models (a) and (d). In the case of model (c), where the fractures are exponentially distributed, they are all concentrated in a small area forming a big cluster. In the current simulation we chose not to allow overlapping between the fractures.

To examine the validity of the algorithm, we present the statistical properties of each distribution in Figs. 3, 4, 5, and 6, respectively. In (a) and (b) of those figures we show the independent probabilities $P(x)$ and $P(z)$ as a function of the x- and z-coordinates of the centres of the fractures, for the daughter distributions (a), (b), (c), and (d) of Fig. 2. The probability plots confirm that the random number generator does create the expected distributions. We also present the two-point correlation functions of the parent spatial distributions, in Figs. 3(c), 4(c), 5(c), and 6(c). We can see that the random uniform distribution has correlations that peak in the middle range, the Gaussian and the exponential peak in the short range, and the Gamma is the most broadband distribution. Thus the ratio of wavelength to correlation length will be greatest for the random uniform distribution, and smallest for the Gamma distribution.

3.2 Power-law or fractal distribution of fracture sizes

In the second example we demonstrate the generation of a fractured network with fractures of variable size. The variation of crack sizes follows a von Kàrmàn correlation function, which gives a power-law or fractal distribution (Wu, 1982). An exponential and a Gaussian correlation function is also available for users to choose. Other functions can also be implemented. The resulting model is shown in Fig. 7(a). We have 150 fractures with a correlation length of 200m, distributed in an 25600 x 2560 m^2 area following a Gamma spatial distribution. The crack size varies from 10m to 250m, and is shown in Fig 7(b) for each one of the cracks. In Fig. 7(c) we present the power spectrum of the size distribution in a log-log scale. The plot shows that the logarithm of the power spectrum varies approximately linearly with the logarithm of the spatial wavenumber. Such a size distribution, is a power-law distribution, often called a fractal (Bonnet et al., 2001).

3.3 Multifracture sets or orientation distributions

There is an option in the program to generate fracture patterns with multiple sets at different orientations or with a given orientation distribution, such

as normal or Gaussian function. In this example shown in Fig. 8, we create a fracture network consisting of three sets and each set has a different orientation. The first set has a uniform spatial distribution, is parallel to the x-direction, and the fracture size varies from 10m to 400m. The second set has a Gaussian distribution, is orientated 30^o from the horizontal, and the fracture size varies from 10m to 200m. The third set has a Gamma distribution, is oriented 60^o from the horizontal, and the size varies from 100m to 600m. We chose each of the set to have different spatial distribution and size in order to represent a case of three different preferential fracture orientations where the difference in the stress conditions generate fractures of different sizes and spatial distributions.

4 Applications

There is an increasing interest in understanding the complicated nature of seismic wave propagation in fractured rocks. Numerical modelling techniques are becoming very common for this purpose and there is a variety of approaches currently available. The algorithm presented here provides a simple, but yet realistic tool to generate fractured rock models that have certain statistical properties and examine how those properties affect the wave propagation in the rock. Such studies may ultimately lead to the extraction of valuable information about the fracture distributions in natural rocks, directly from seismic data. The synthetic patterns generated using this simple method may be potentially used for a range of applications. Here we just list three cases where we have used the synthetic fracture patterns for various applications (details of these can be found in our companion papers).

a) The generated fracture patterns can be compared with real fracture patterns to understand the rock mechanics of natural fractures and to study the statistical properties of natural fractures (Main et al., 1990).

b) The synthetic fracture patterns can be used to study the seismic wave propagation in fractured rock (Liu et al., 2001). In a separate paper, We present some results of numerical modelling using the pseudospectral method. We use the models presented in Fig. 2, put a source in the center of the model and take snapshots at consecutive time steps. A sample snapshot is shown in Fig. 9. The algorithm was used by (Vlastos et al., 2003) to simulate fractured rock, and study the effects of spatial distribution of cracks and their sizes.

c) These synthetic fracture patterns can be used in an existing fluid flow simulator to study the effects of various fracture distributions on fluid flow in fractured rock. An example has been given in our companion paper (Vlastos et al., 2003).

5 Summary

Understanding the response of the rock to seismic waves is an important issue in exploration geophysics. Fracturing is making things more complicated and a good representation of the fractured network is needed for a complete study of the effects. We presented an algorithm that uses a simplified approach to the generation and evolution of the network of cracks. The algorithm is a useful tool for the creation of sets of cracks that have statistical properties of our choice. It has been used successfully for wave propagation studies. The code is written in standard FORTRAN 77, and is available from the author (E.Liu@bgs.ac.uk).

6 Acknowledgments

We thank our colleagues Ian Main, Patience Cowie, and Peter Leary for useful discussion about fracture scaling and distributions in nature. This research was supported by British Geological Survey, and the sponsors of the Edinburgh Anisotropy Project (EAP). Part of this work was done while the first author was a visiting scientist (December 2001) at the Institute of Geology & Geophysics, Chinese Academy of Sciences, funded by the National Natural Science Foundation of China (No. 49928403). This work was published with the permission of the Executive Director of the British Geological Survey (NERC) and the EAP Sponsors.

References

An, L.-J. & Sammis, C.G., 1996. A cellular automaton for the development of crustal shear zones, *Tectonophysics*, **253**, 247-270.

Bonnet, E., Bour, O., Odling, N.E., Davy, P., Main, I.G., Cowie, P. & Berkowitz, B., 2001. Scaling of fracture systems in geological media, *Review of Geophysics*, **39**, 347-383.

Cowie, P., Vanneste, C. & Sornette, D., 1993. Statistical physics model for the spatio-temporal evolution of faults, *J. Geophys. Res.*, **98**, 21,809-21,821.

Cowie, P., Sornette, D. & Vanneste, C., 1995. Multifractal scaling properties of a growing fault population, *Geophys. Journ. Int.*, **122**, 457-469.

Cruden, D.M., 1977. Describing the size of discontinuities, *Int. J. Rock Mech. Min. Sci.Geomech. Abstr.*, **14**, 133-137.

Dershowitz, W.S. & Einstein, H.H., 1988. Characterizing rock joint geometry with joint system models, *Rock Mech. Rock Eng.*, **21**, 21-51.

Hentschel, H. G. E. & Proccacia, I., 1983. The infinite number of generalised dimensions of fractals and strange attractors, *Physica D*, **8**, 435-444.

Liu, E. & Zhang, Z.J., 2001. Numerical study of elastic wave scattering by distributed cracks or cavities using the boundary integral method, *J. Comp. Acoust.*, **9**, 1039-1054.

Main, I. G., 1996. Statistical physics, seismogenesis, and seismic hazard, *Rev. Geophys.*, **34**, 433-462.

Main, I.G., Peacock, S. & Meredith, P.G., 1990. Scattering Attenuation and the Fractal Geometry of Fracture Systems, *Pure Appl. Geophys.*, **133**, 283-304.

Narteau, C., Shebalin, P., Holschneider, M., Le Mouël, J.L. & Allègre, C.J., 2000. Direct simulation of the stress redistribution in the scaling organization of fracture tectonics, *Geophys. J. Int.*, **141**, 115-135.

Press, W. H., Teukolsky, S. A., Vetterling, W. T. & Flannery, B. P., 1997. *Numerical Recipes in Fortran 77: The Art of Scientific Computing*, Cambridge University Press, 266-283.

Sornette, D. & Sornette, A., 1999. General theory of the modified Gutenberg-Richter law for large seismic moments, *Bull. Seismol. Soc. Am.*, **89**, 1121-1130.

Vlastos, S., Liu, E., Main, I.G. & Li, X.-Y., 2003a. Numerical simulation of wave propagation in media with discrete distributions of fractures: effects of fracture sizes and spatial distributions, *Geophys. J. Int.*, in press.

Vlastos, S., Schoenberg, M., Maillot, B., Main, I.G., Liu, E. & Li, X.-Y., 2003b. Fluid flow simulation in a fractured medium: effects of pore pressure changes on seismic waves, *Expanded Abstracts, EAGE Ann. Int. Meeting., Stavanger*.

Wu, R.S., 1982. Attenuation of short period seismic waves due to scattering, *Geophys. Res. Lett.*, **9**, 9-12.

FIGURE CAPTIONS

Figure 1. Flow chart of the algorithm used to generate the four spatial distributions of fractures shown in Fig. 4.

Figure 2. The four different models, illustate different statistical distributions of fractures: (a) random uniform, (b) Gaussian, (c) exponential, and (d) Gamma.

Figure 3. Statistical properties of the random uniform distribution of fractures in Fig. 4(a). (a) Probability plot of the coordinate of the centre of fractures along the x-direction, (b) Probability plot of the coordinate of the centre of fractures along the z-direction, (c) Two-point correlation function of the parent distribution of fractures.

Figure 4. Statistical properties of the Gaussian distribution of fractures in Fig. 4(b). (a) Probability plot of the coordinate of the centre of fractures along the x-direction, (b) Probability plot of the coordinate of the centre of fractures along the z-direction, (c) Two-point correlation function of the parent distribution of fractures.

Figure 5. Statistical properties of the exponential distribution of fractures in Fig. 4(c). (a) Probability plot of the coordinate of the centre of fractures along the x-direction, (b) Probability plot of the coordinate of the centre of fractures along the z-direction, (c) Two-point correlation function of the parent distribution of fractures.

Figure 6. Statistical properties of the Gamma distribution of fractures in Fig. 4(d). (a) Probability plot of the coordinate of the centre of fractures along the x-direction, (b) Probability plot of the coordinate of the centre of fractures along the z-direction, (c) Two-point correlation function of the parent distribution of fractures.

Figure 7. (a) Fracture distribution with power-law distribution of fracture sizes. (b) Illustration of the sizes of fractures in model (a), that follow a power-law distribution. (c) Power spectra of fracture size distributions shown in (a). (d) Cumulative number of the fractures of model (a) plotted against the fracture size.

Figure8. Three sets of fractures with different orientations.

Figure9. Snapshots taken at t=250 ms. (a) to (d) correspond to fracture distributions (a) to (d) in Fig. 2. The numbers on the top and on the left side of the snapshots are the actual model sizes.

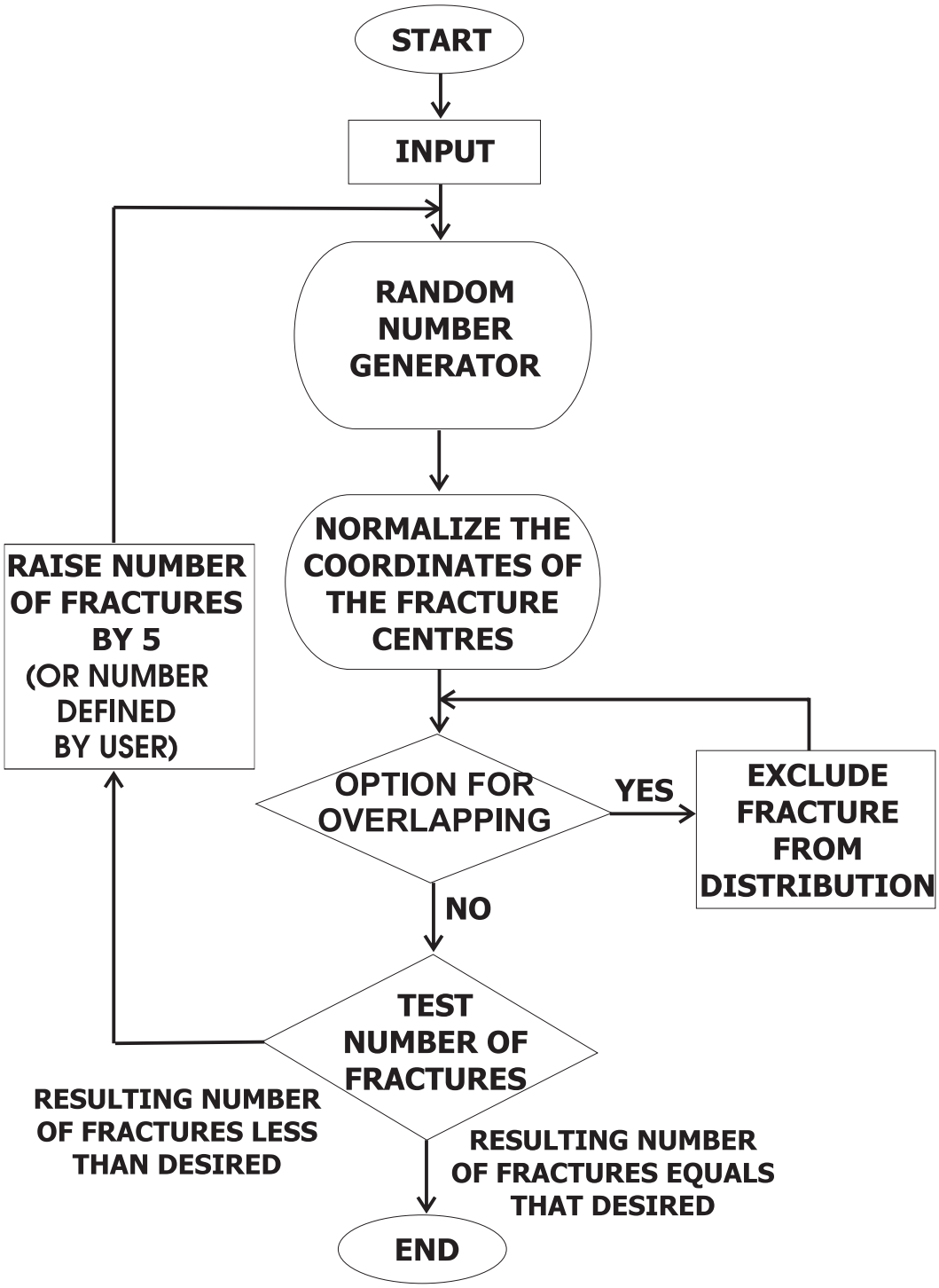
START
INPUT
RANDOM NUMBER GENERATOR
NORMALIZE THE COORDINATES OF THE FRACTURE CENTRES
OPTION FOR OVERLAPPING
YES
EXCLUDE FRACTURE FROM DISTRIBUTION
NO
TEST NUMBER OF FRACTURES
RESULTING NUMBER OF FRACTURES LESS THAN DESIRED
RAISE NUMBER OF FRACTURES BY 5 (OR NUMBER DEFINED BY USER)
RESULTING NUMBER OF FRACTURES EQUALS THAT DESIRED
END

Figure 1

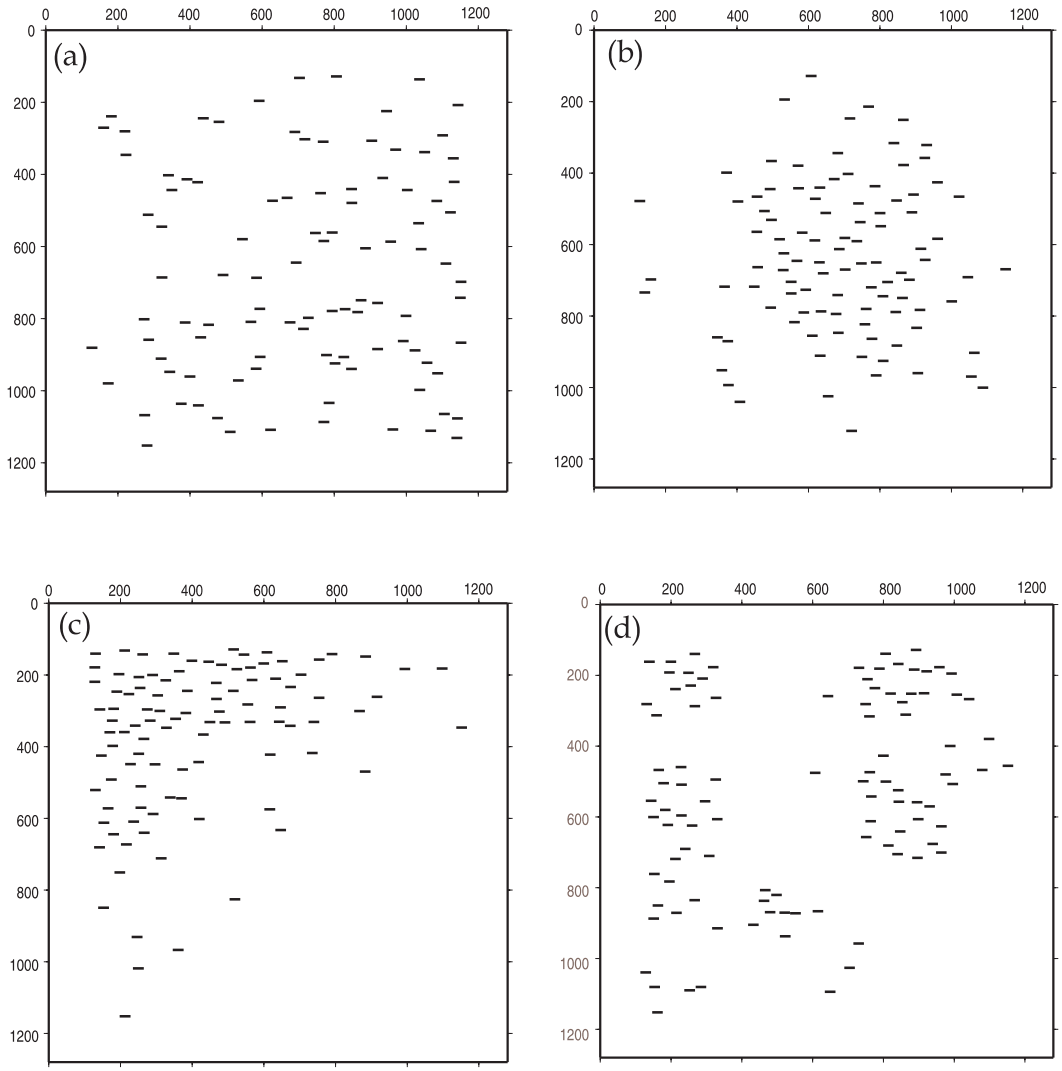

Figure 2

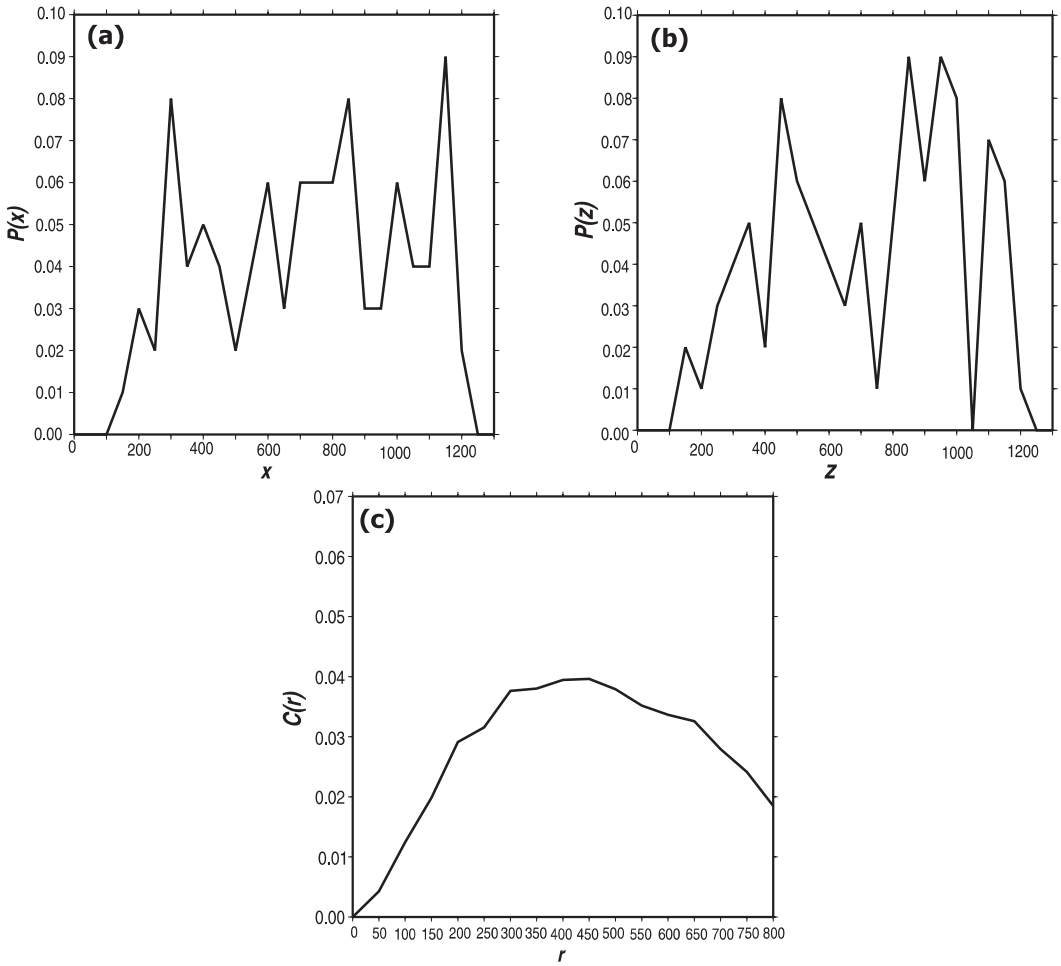

Figure 3

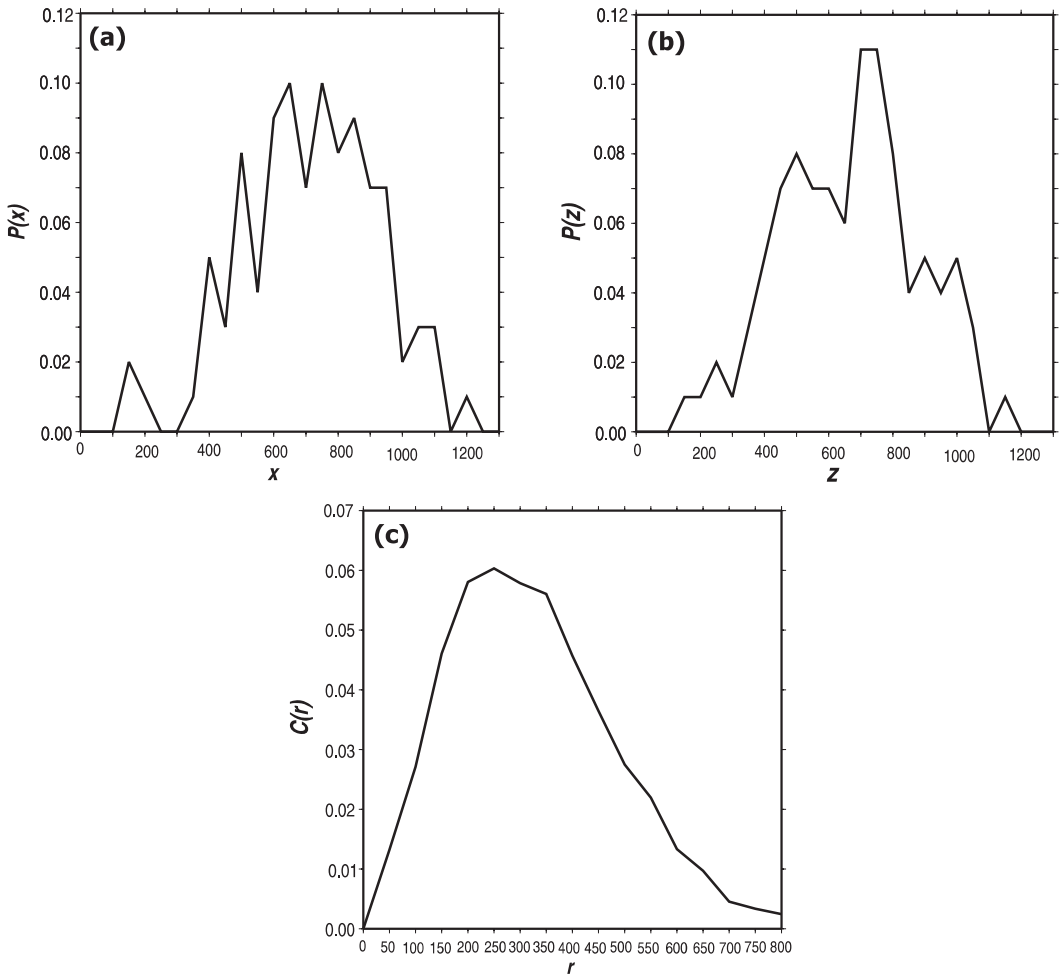

Figure 4

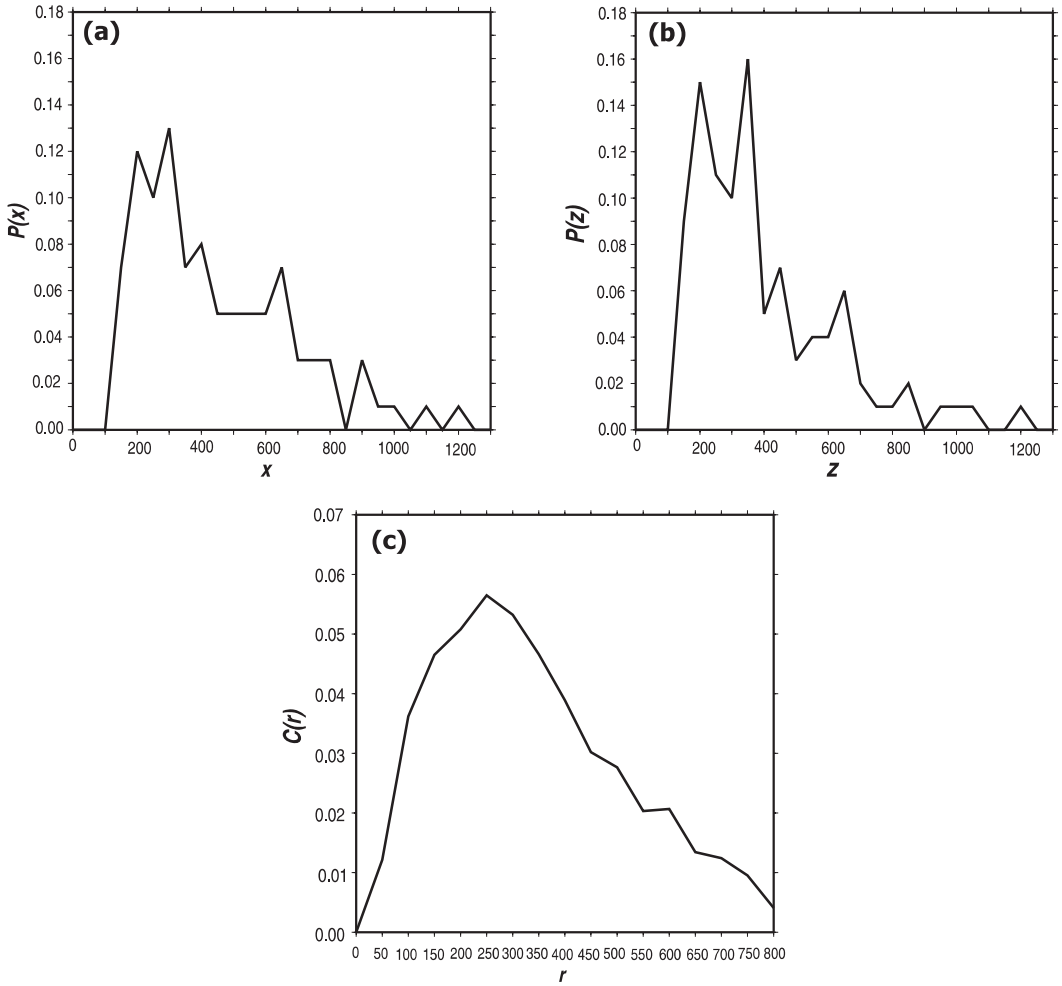

Figure 5

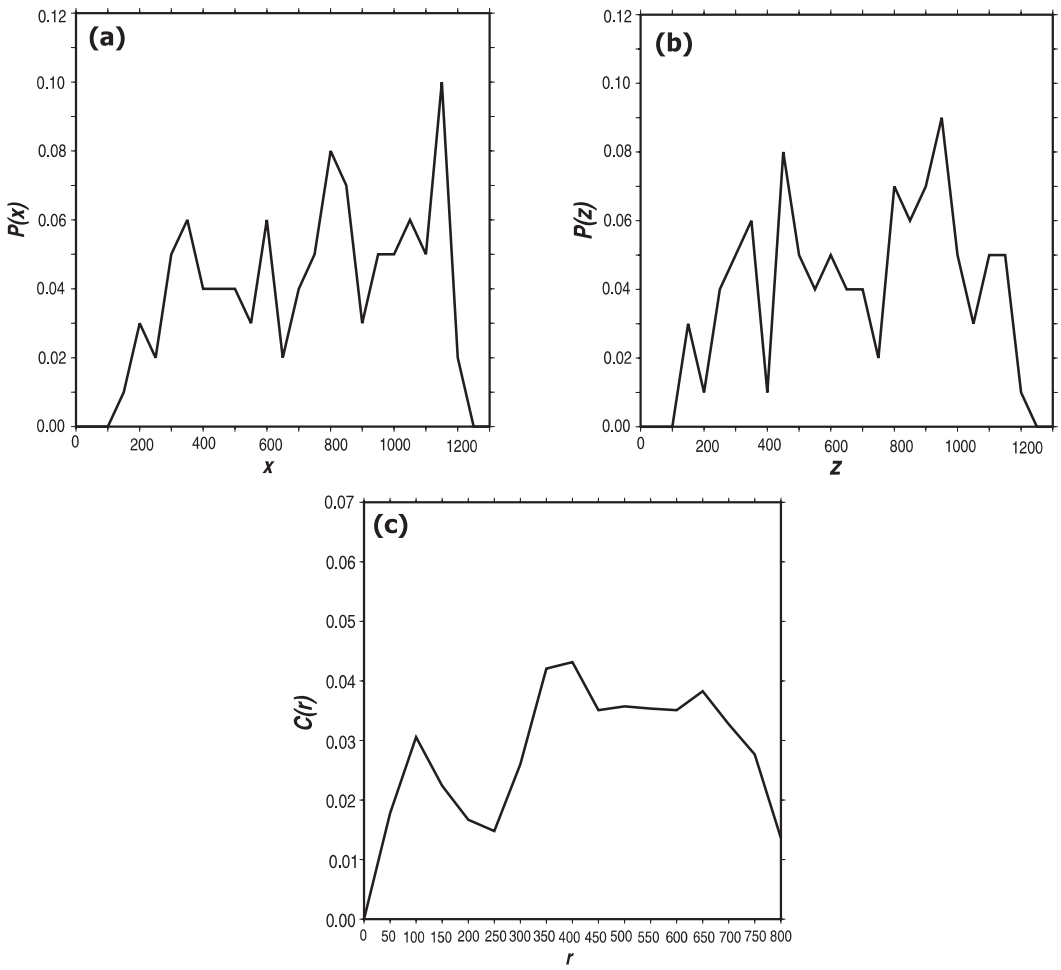

Figure 6

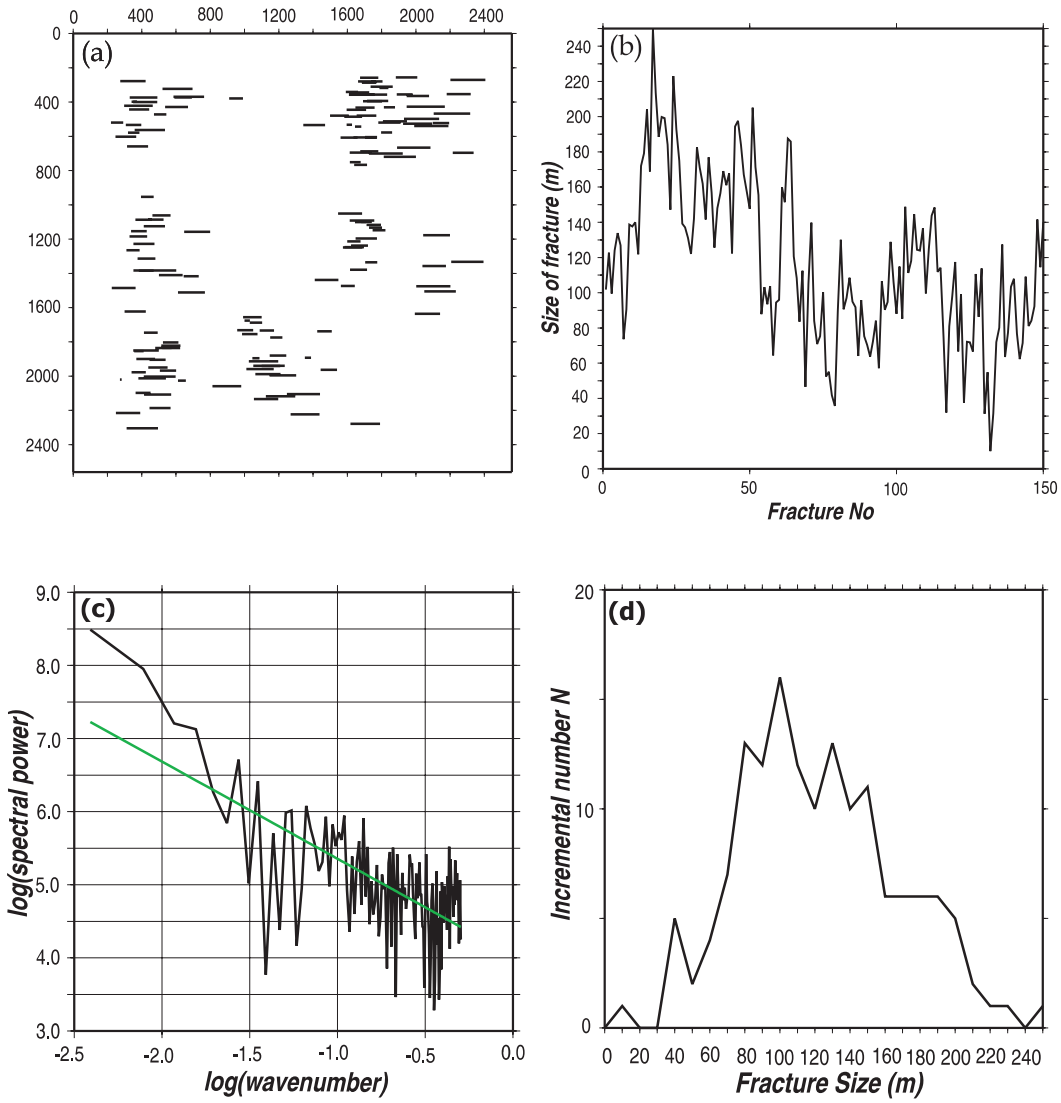
(a)
(b)
Size of fracture (m)
Fracture No
(c)
log(spectral power)
log(wavenumber)
(d)
Incremental number N
Fracture Size (m)

Figure 7

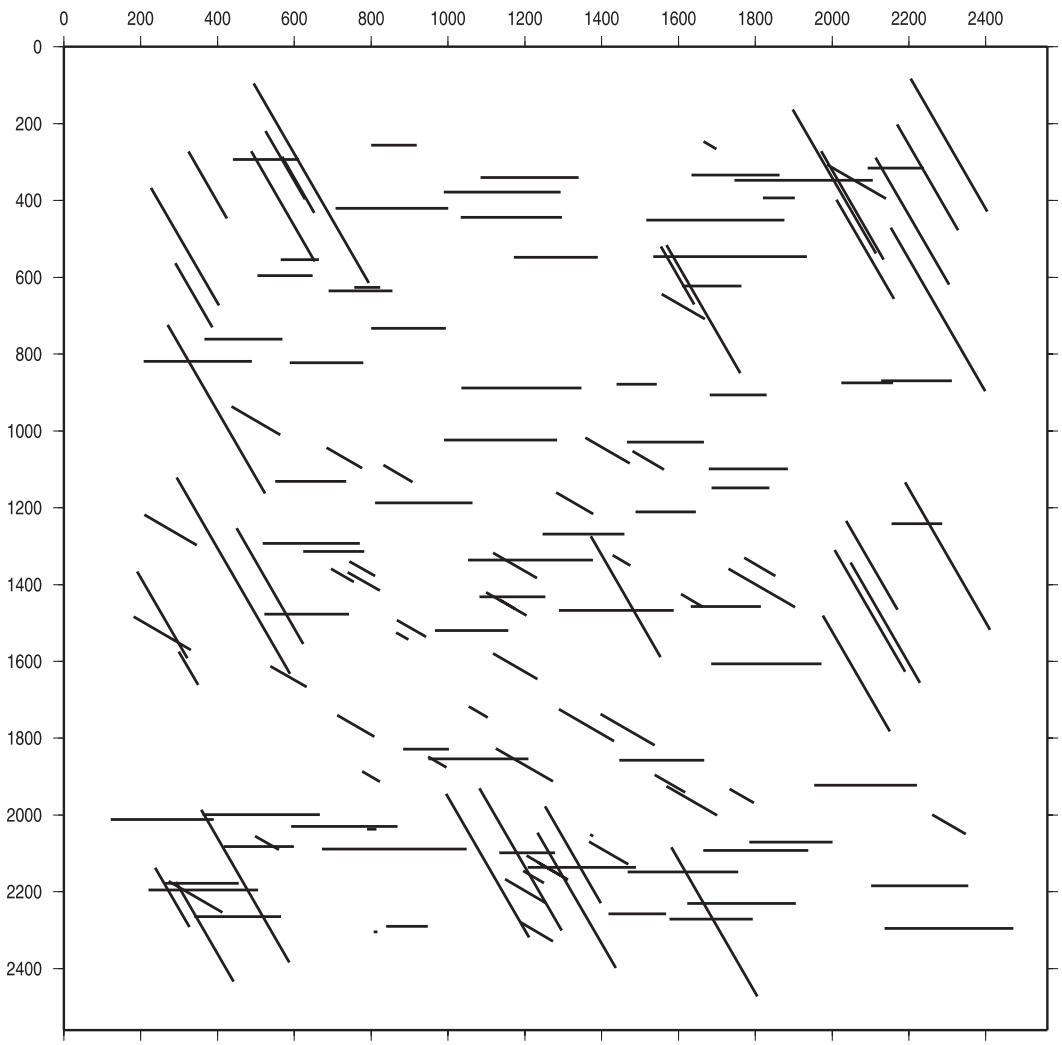

Figure 8

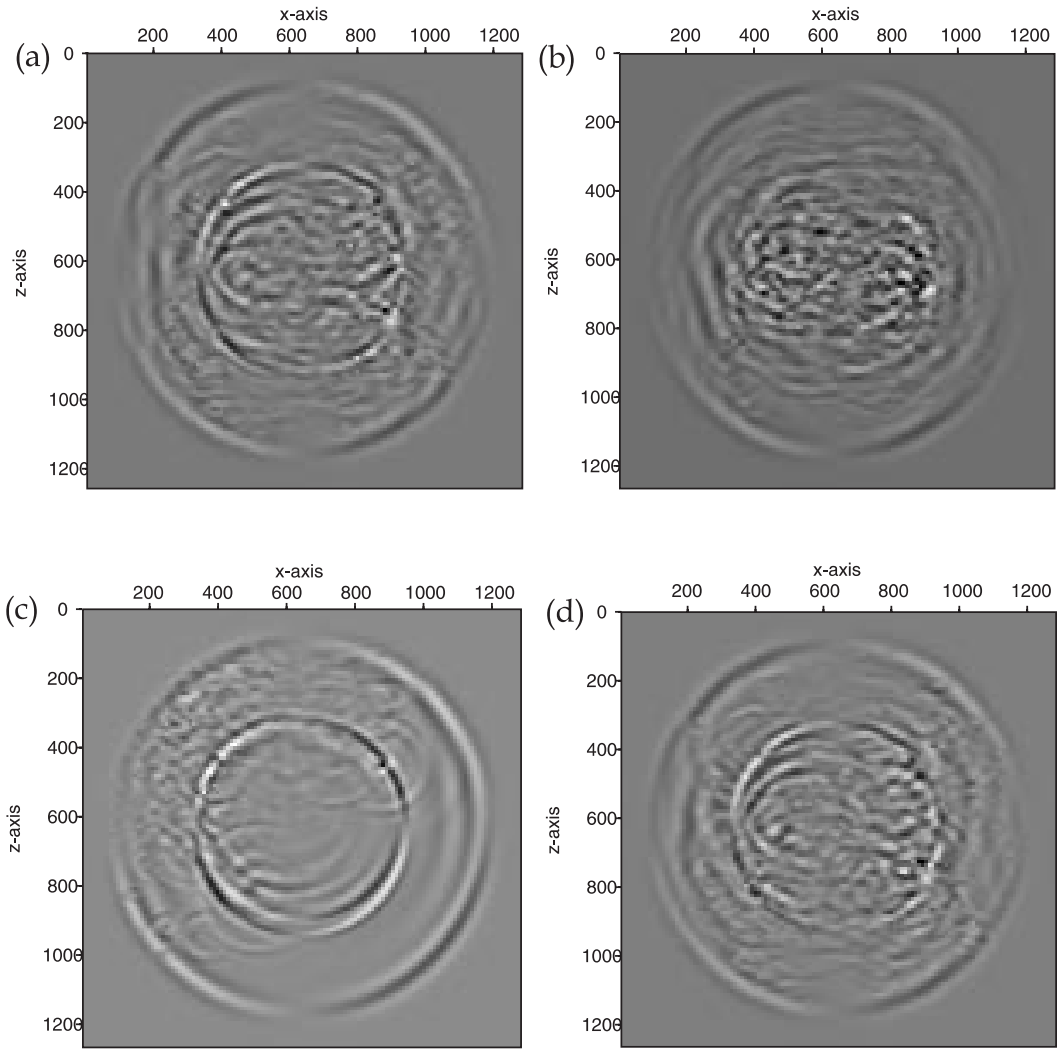

Figure 9